



## Nano-structured Thin Films for Hydrogen-Permeation Barrier Applied on AISI 1018 Steel Used in Petroleum Applications

Neam F. Mohammed, Baha S. Mahdi\* , Amin D. Thamir

Production Engineering and Metallurgy Dept., University of Technology-Iraq, Alsina'a street, 10066 Baghdad, Iraq.

\*Corresponding author Email: <mailto:baha.s.mahdi@uote>

### HIGHLIGHTS

- A third coating layer gives an acceptable adhesion force with the highest deposition rate.
- Nano-structured coating increased bulk AISI 1018 steel tensile strength after the hydrogen charging process.
- Double layer of Ti and  $TiO_2+Al_2O_3$  coat gives a 20 percent increase in tensile strength after HC for AISI 1018 steel.
- The layer of ceramic coatings  $TiO_2$  with  $Al_2O_3$  as coating Nano-structured thin films can improve the hydrogen permeation resistance
- The Nano titanium layer showed the main portion in bonding

### ABSTRACT

Hydrogen embrittlement is a diffusible Hydrogen that is harmful to the toughness of iron. It follows, therefore, that the harmful influence of diffusible Hydrogen can be mitigated by preventing its entry into steel. This approach was achieved by using three coating layers as a coating nanostructure thin layer by DC sputtering on steel structural (AISI 1018) and hydrogen charging (HC) effect on uncoated and different Nano coated tensile specimens. The first layer was Titanium as a bonding layer, the second layer was  $TiO_2$  with  $Al_2O_3$ , and the third layer was  $Al_2O_3$ . Using a titanium Nano layer coating on AISI1018 steel tensile specimens increased the tensile strength from 570 to 659 MPa with 16 hours of charging, which is considered a good increase. In contrast, the elongation remained in a steady-state with little difference in values compared to changing the charging time and the coating of the double layer. Furthermore, it was found that samples coated with  $TiO_2$  and  $Al_2O_3$  by the DC method had advanced hydrogen embrittlement resistance and increased tensile strength (from 565 to 680 MPa with 8 hours of charging process). Moreover, the maximum adhesion value was related to the triple layer at 596 psi, and the lowest value was 309 psi using the titanium layer alone. The coating time was 5 hours of the sputtering process for all specimens. The coating layers are considered a good barrier for hydrogen permeation through steel structures (AISI 1018).

### ARTICLE INFO

**Handling editor:** Omar Hassoon

#### Keywords:

DC sputtering; hydrogen permeation; hot filament Hydrogen charging; Nano-structured; hydrogen embrittlement.

### 1. Introduction

Hydrogen-aided mechanical degradation of structural materials is one of the most complex phenomena of metallic materials deprivation due to several original unknowns in the degradation procedure kinetics linked to the degradation in the absenteeism of Hydrogen in metal.

In particular microstructures and alloys, hydrogen atoms may dissolve in iron and steel alloys and display distinctive features including mutability, solubility, and diffusivity. Metals like lead and steel that are mechanically active can suffer catastrophic destruction from hydrogen [1, 2]. One of the most frequent issues in the petroleum sector is pipeline damage failure brought on by corrosion, especially pipes for transmission lines that were submerged or buried in the ground or water. As a result, they are regarded as the largest engineering challenges, the most pervasive in the globe, and are most notable for having a considerable impact on those projects. [3] Is cathode overprotection of the reduction of water molecules. Corrosion is one of the greatest shared problems in the petroleum sector, especially in transmission pipelines buried or submerged in water or soil. Thus, it is most famous for the significant influence of these complications on those plans, as measured as the major engineering problems in the economy and the most general in the world [4, 5].

The climate variation of the Iraqi environment also means many erosion areas which are pretentious on corrosion projects. These projects contain thousands of kilometers of pipeline transporting natural gas, petrol portions, and crude oil, and

additional schemes under the earth's surface for ground boilers equipped for loading [6]. The steel was one of the main materials of carbon steel used for pipeline conveyance of fuel due to its physical, mechanical, and low cost. However, this material is highly affected by corrosion where environmental circumstances play an important role, especially in the external corrosion of the oil pipeline. Other factors influencing mild steel corrosion rate include the content of the petroleum product passing through it, moisture, temperature, pH, and soil type [7, 8].

Surface barriers can retard hydrogen entry into the substrate metal by virtue of their diffusivity and low hydrogen solubility. Metal surface coatings can potentially modify the surface properties, including the adsorption, metal surface catalytic responses, or through mixtures of these features [9]. The HE, by the method of one of the instruments of hydrogen destruction, is the deprivation of the motorized properties of damage to ductility, tensile strength, metals, and other materials. It typically reduces fracture resistance and sub-criticality, especially due to melted Hydrogen's attendance. The hydrogen embrittlement of structure iron, steel, and their alloys is a very stimulating phenomenon since these materials are extensively used in many industrial applications, while practically applicable predictive physical perfection and a fully developed product still do not exist [10,11].

Modern studies have identified hydrogen-enhanced de cohesion (HEDE) [12,13] and hydrogen-enhanced localized plasticity (HELP) as two mechanisms responsible for hydrogen embrittlement [14, 15] in many non-hydride starting metals. The coating processes offer defense to construction surfaces uncovered by near-destructive and corrosion surroundings in many fields. Therefore, care is essential and aimed at application [16]. Various nanomaterials are used as layer nano-coating in petroleum manufacturing, such as TiO<sub>2</sub>, Al<sub>2</sub>O<sub>3</sub>, and SiO<sub>2</sub>. Amongst nano-coatings using TiO<sub>2</sub>, TiO<sub>2</sub> is considered the most common corrosion protection layer due to its unique chemical, optical, and electrical properties [17]. Deyab and Keera [18], explored 1.0 M H<sub>2</sub>SO<sub>4</sub> corrosion prevention for carbon steel using a coating system containing nano-TiO<sub>2</sub> particles of varying sizes (i.e., 10, 50, 100, and 150nm). These nano-TiO<sub>2</sub> particles increased the corrosion resistance of coatings. In 2015 Eguchi, and Tamura [19] Stated that coating with Al<sub>2</sub>O<sub>3</sub>, TiC, or TiN reduced the hydrogen permeability of the 316L austenitic stainless steel twice as much as the uncoated substrates, Xinfeng Li and others in 2019 studied the action of surface roughness on the hydrogen blistering in steel, It was found that ground surfaces that have greater roughness showed compressive residual stress in compression to polished surfaces the ground test specimens offers less sensibility to hydrogen blisters compared with the polished test specimens[20]

In 2020 Wasim and Djukic [21] studied the influence of hydrogen penetration of low-carbon steel at macro-, micro-, and nanoscales in the hydrogen-rich acidic atmosphere. The results proved that there is a directly proportional relationship between the concentration of hydrogen and corrosion rate with increasing charging time,

The present investigation aims an increasing the tensile strength of coated AISI 1018 steel by about 30% after the hydrogen permeation process leading to a raise in the intrinsic bulk material properties without applying heat treatment used in petroleum applications. In addition, the study will apply nano-coat layers of materials that resist or reduce hydrogen permeation, which causes embrittlement in AISI 1018 steel pipes. Also, an examination of the effects of single or multiple Nano coats on hydrogen embrittlement will be performed.

## 2. Experimental Work

### 2.1 Base Metal Selection

A chemical analysis was conducted to determine the elements' composition and the type of steel using an OE Thermo ARL 3460 spectrometer. Table 1 shows the elements of the used steel and their proportions. The chemical composition weight ratio of carbon has a value of (C = 0.18%). This means that the steel used was (Low Carbon Steel) (L.C.S.) [22]. Therefore, according to the chemical analysis, the nearest steel designation is AISI1018.

**Table 1:** Composition of AISI 1018 as tested using optical emission device

<i>Tested result</i>	<b>Alloying Element</b>	<b>C</b>	<b>Si</b>	<b>Mn</b>	<b>Cr</b>	<b>S</b>	<b>MO</b>	<b>Fe</b>
	Wt.%	0.181	0.223	0.758	0.0956	0.0342	0.01	98.698

### 2.2 Prepare The Target Coating Method and The Substrate

Targets used in the sputtering process prepared from compressed metal powders are devoid of the need for a sintering procedure, as shown in Figure 1. These targets' compositions are explained in Table 2. For example, the Titanium target is made of 20 grams of titanium powder with an average grain size of 46m. Manufacturing a target consists of pressing it into cylindrical stainless steel with a diameter of 50mm and a thickness of 5mm. The pressing was done using a hydraulic press of 50 MPa with a pressing time of 10 minutes. The final dimensions of the produced target were 5 cm in diameter and 2.6mm in thickness.

**Table 2:** The composition of the two powder-compacted targets

<b>Target No.</b>	<b>Composition of target powders (W %)</b>
1	Titanium powder (100%)
2	Titanium (70%) Aluminum (30%)
3	Aluminum (100%)

The Titanium and Aluminum targets were made by mixing 14 grams of titanium powder with 6 grams of aluminum powder using a magnetic stirrer device for 20 minutes. The mixed powder was compacted in the same manner used to make titanium targets, and the final target thickness was 3mm. The target was made of aluminum powder done in the same manner mentioned for the above two targets, as shown in Figure 2. It is important to know that these targets are handled carefully because they are not sintered.

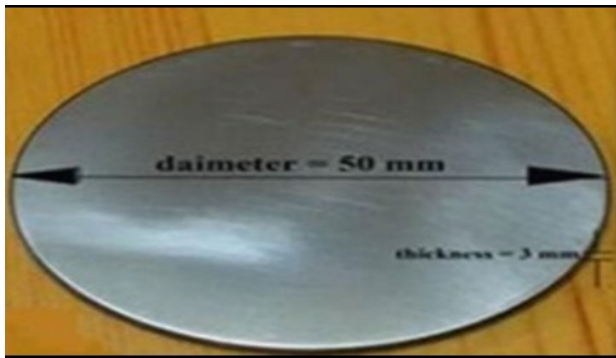


Figure 1: Titanium Target after compaction



Figure 2: Aluminium target after extracted from S.S. dye mold

### 2.3 Design of The Tensile and Adhesion Test Specimens for The Charging Process

To evaluate the mechanical properties of the charged steel samples, tensile test specimens were prepared according to the sub-size specimen dimensions mentioned in ASTM E8 [23]. Figure 3 shows the manufactured steel specimens. The adhesion specimens' dimensions were (30×40×2) mm.

The vacuum arrangement consists of a turbo pump (V-1000HT) aided by a hydraulic rotary pump (60 m<sup>3</sup>/h, Blazer). In addition, a setting up of Pirani gauges (LH-Thermo vac with Combitron CM350) and Edward CP25-K with controller 1102) in the plasma chamber was requisite to display the actual and partial pressure of the discharge gases.



Figure 3: The manufactured AISI 1018 steel specimens according to ASTM-E8

### 2.4 Coating Process

The DC sputtering technique was achieved using a low-pressure argon discharge device gas involving an evacuated chamber, an anode disk of stainless steel, and the target (cathode). The cathode facing the anode also provides the gas discharge by an electrical field with a 4 kV power supply DC. The cathode electrodes' bottommost variation was protected via the insulator disk (ceramic) and a tube made of quartz. The diameter of the top electrodes was 14.5 cm, while the target electrode was 7.5 cm. The distance between them was 4cm. The gas source-flow controller system is accountable for supplying the feedstock at the wanted flow rate and gas pressure to the plasma chamber. It consists of double-stage regulators, tubing, and fittings for the gas storage cylinders (Argon). In addition, a dual-stage needle valve regulated the movement pressure of the plasma chamber. Figure 4 shows the device component and its working principle.

After completing the sputtering process, specimens faced side to target colored in a rainbow spectrum where the red color represents the thicker region. Also, the violet color represents thinner regions in specimen ends. This presentation is shown clearly in Figure 5.

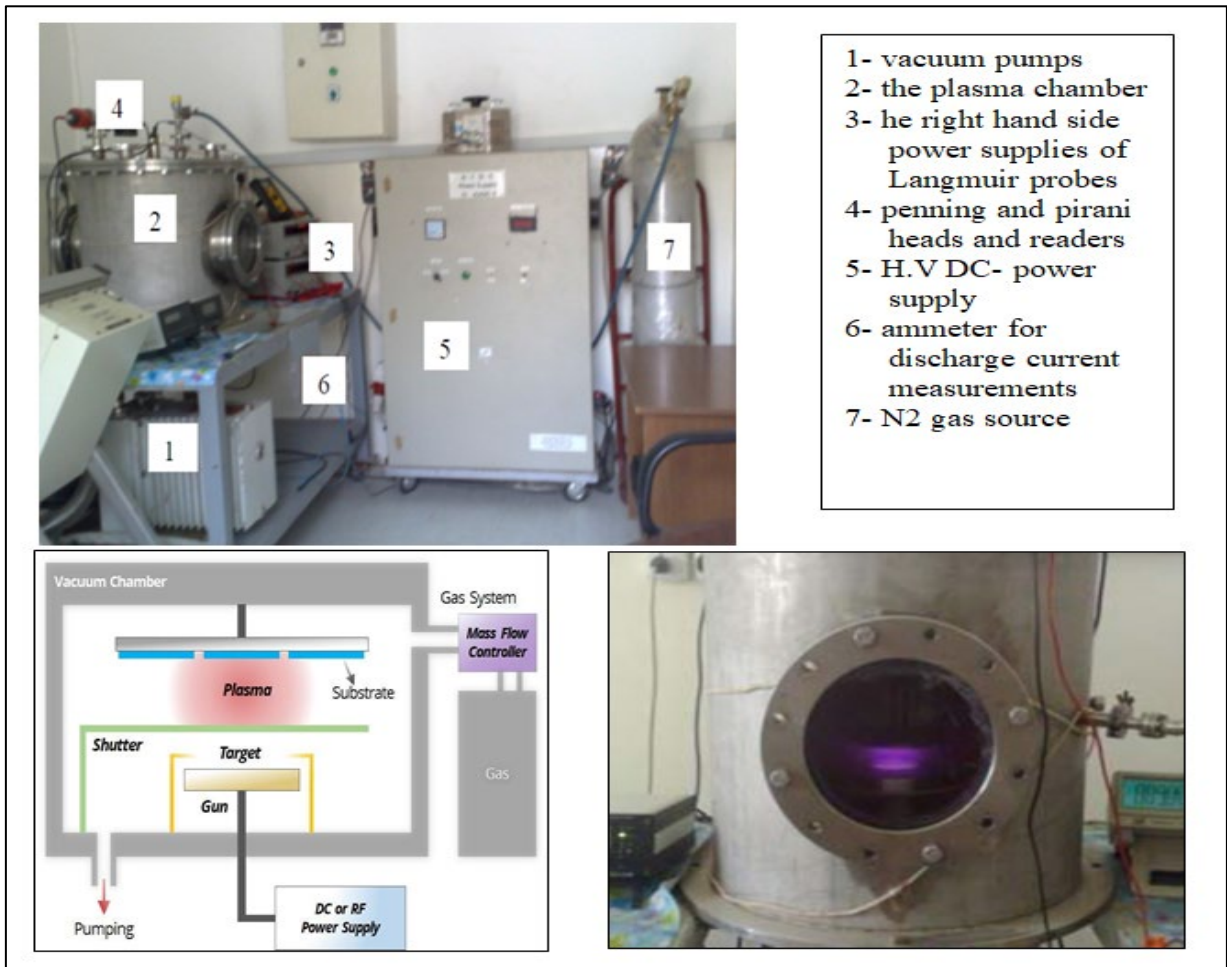


Figure 4: The DC sputtering device used for coating components, plasma glowing in the chamber, and the schematic principle of work for the device



Figure 5: The tensile specimen after the coating process

### 2.5 Applying of Coating Layers - Single Layers Ti And Double Layer (TiO<sub>2</sub>+Al<sub>2</sub>O<sub>3</sub>)

A substrate of low-carbon steel AISI1018 was coated with a thin layer of Titanium as a bonding layer with working conditions. Thin films were deposited on substrates using TiO<sub>2</sub>+Al<sub>2</sub>O<sub>3</sub> targets. with low pressure of Argon + Oxygen gasses with a flow rate of 20 SCCM. Thin films were deposited on substrates of steel L.C.S by Al target, which its composition was a powder (100w%) of aluminum by reactive low-pressure oxygen 20% Argon 80%, as tabulated in Table 3.



**Table 3:** The condition of the substrate of the steel ASTM A29 Grade 1018 was layered with three coated layers

Layer	Time\hour	sputter Pressure\mbar	Voltage V	Current mA	Power\W	Temp\°C	Gas flow rate Secm
Ti	5	$6 \times 10^{-2}$	1400	22	30.8	198	Ar
TiO <sub>2</sub> +Al <sub>2</sub> O <sub>3</sub>	5	$8 \times 10^{-2}$	1400	22	30.8	204	70 Ar+30 % O <sub>2</sub>
Al <sub>2</sub> O <sub>3</sub>	5	$6 \times 10^{-2}$	1400	22	30.8	200	80 Ar+20%O <sub>2</sub>

## 2.6 Preparation of A Hydrogen Permeation Solution

In this work, a 0.5M concentration of H<sub>2</sub>SO<sub>4</sub> in distilled water was prepared as a hydrogen generator solution, as shown in Figure 6. In addition, 15% alcohol was added to the solution as an inhibitor to hydrogen gas bubbles generated on the cathode to prevent decreasing electrical current applied by the DC power source where the tensile specimen was located as the cathodic pole.

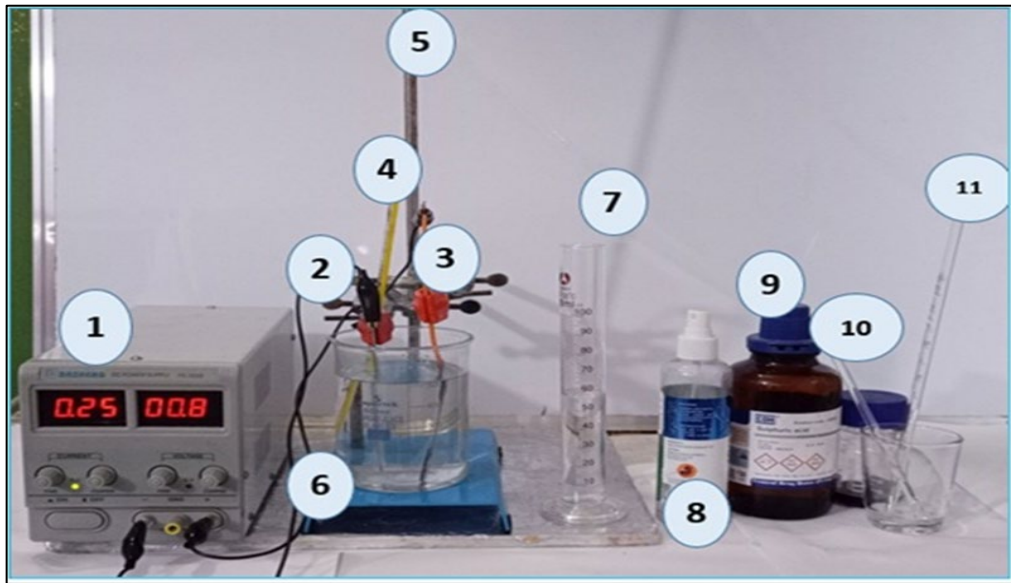


**Figure 6:** Charging electrolytic system used to do the Hydrogen permeation process for tensile test specimens. 1- power supply, 2- electrode metal 3- tensile test specimens of Hydrogen permeation, 4- thermometer, 5- fixed stand, 6- Beaker, 7- Distilled water in Cylinder, 8- Alcohol 75%, 9- H<sub>2</sub>SO<sub>4</sub> pure 98%, 10- Stirrer, 11- pipette

## 2.7 Cathodic Charging Setup

Cathodic or Hydrogen charging was done using an electrolyte circuit by making the structural carbon steel A29 tensile test specimen a cathode. The anode pole was stainless steel (150×20×2) mm. Before the charging process, the tensile specimen was connected to copper wire by discharge welding from one side and coated using epoxy resin from all sides except the gage length of one side opposite the anode face. The exposed facade of the specimen's area is fixed with (≈230) mm<sup>2</sup> to ensure standardization of the current density and make it a known variable. Also, the charging process includes 500 ml Bicker filled with an acidic electrolyte of 0.5M of H<sub>2</sub>SO<sub>4</sub> in distilled water and 5-10% Alcohol as an inhibitor to form hydrogen bubbles covering the cathode pole in most cases. To ensure the correct electrolyte concentration, 56 ml of 98% Sulfuric acid mixed with 450 ml of distilled water and 75 ml of alcohol is added before the charging process is started. The charging process is done by immersion of a partially coated tensile specimen as the cathode, and stainless steel plate as the anode in an acidic electrolyte with a distance between them filled beaker of about 6cm. A direct current power supply was set to 0.8 volts, and the current was around 0.25 ampere. So, the current density was derived by dividing the power supply current by the exposed tensile test specimen area, and the current density value was (1.08) mA. The charging time varied from 4 to 16 hours. These time intervals were chosen upon the change in mechanical properties found during tests. Therefore, it can be said that the charging time builds on trial and error for many samples until they reach reasonable results and are predicted in literary works.

## 2.8 Adhesive Test

The device's working theory is the concept of two surfaces sticking together due to molecular attraction towards one another. AUS machine, available at the National Center for Packing and Packaging-Ministry of Industry and Minerals, was used to examine the low-carbon steel samples. It is a device made up of Dali. It is installed on the surface of steel samples coated with a strong adhesive material (epoxy adhesive). The piston separates the coat from the surface of the low-carbon steel sample and shows on the screen the force necessary for the separation process (adhesive strength), as shown in Figure 7.



Figure 7: Adhesive strength examination device

### 3. Results and Discussion

#### 3.1 SEM Measurements

To ensure coating measurements and their amounts like coating thickness and morphology for different specimens a scanning electron is difficult to prepare conventional standard cross-sectional specimens for SEM test due to the very thin layer thickness and removing it by specimen preparation steps such as grinding, polishing and chemical etching, therefore another method used to indicate thin coat by scratching the coated surface with very sharp tool gently and this area enlarged using SEM imaging to indicate fragmented coat pieces which located normal to scanning surface and measuring its thickness where this way is the best method to detect nanoscale coat dimensions. Figure 8 shows the titanium thin layer thickness of about (50 to 100) nm.

As seen in Figure 8 the titanium coat is hard and sound without porosity and it is known that titanium has good resistance to hydrogen permeation so it can be told that this process represents a successful process to protect steel from hydrogen embrittlement effect but this will be discussed later in hydrogen charging tests by applying rich atomic hydrogen environment of coated specimens surfaces.

For the double layer coating as in Figure 10, the coating thickness increased to about (300) nm as it tested in the same manner done for steel specimens coated with titanium layer in Figure 8.



Figure 8: SEM image of Ti thin layer coating at a - 37kx b – 100kx

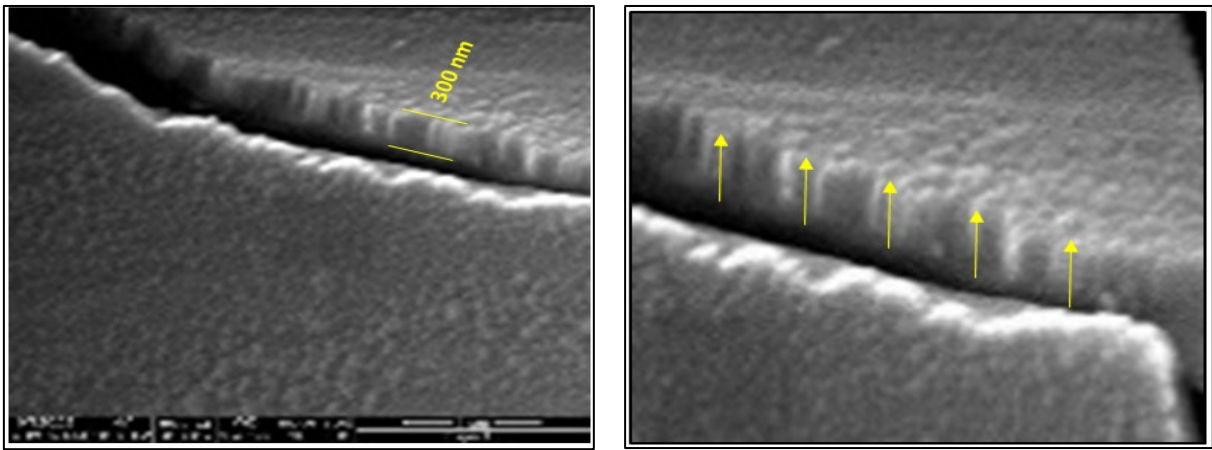


Figure 9: a - SEM image of a thin scalped layer of 0.7Ti+0.3Al target at 70kx. b- same surface but with a magnification of 300kx

Although with a thicker coating of the double layer shown in Figure 9 compared to the single layer but the morphology of images indicates a rougher dendritic structure.

By three layers, the coating thickness as shown in Figure 10 the thickness reach about (500) nm. All three coating shows uniform sound coat without porosity complying with adhesion test and fracture mechanism indicating hard brittle coats without ductile deformation.

### 3.2 Effect of Hydrogen Charging on Steel Strength

Three samples of uncoated AISI 1018 steel were charged at different times, as shown in Figure 11. The tensile strength decreased from 550 to 490 (MPa) and yield strength values with charging time at the same rate. But, elongation values varied. This proves that the longer the hydrogen embrittlement time, the lower the mechanical properties values.

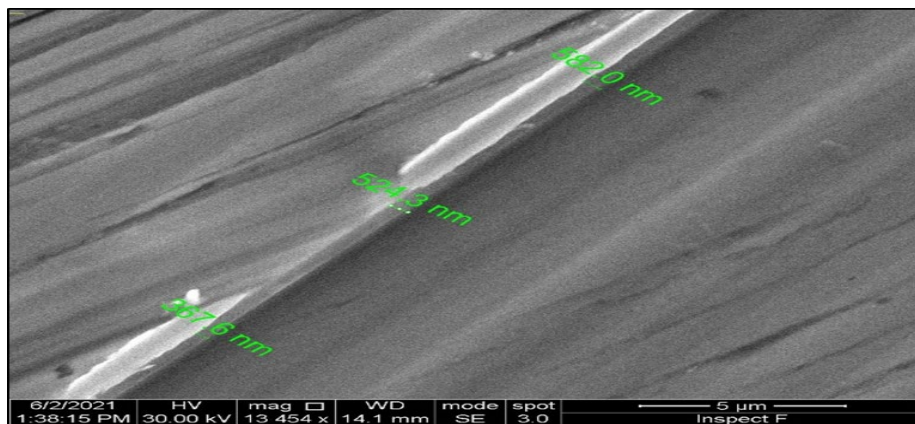


Figure 10: SEM image of triple layer  $Ti+(TiO_2+Al_2O_3) + Al_2O_3$

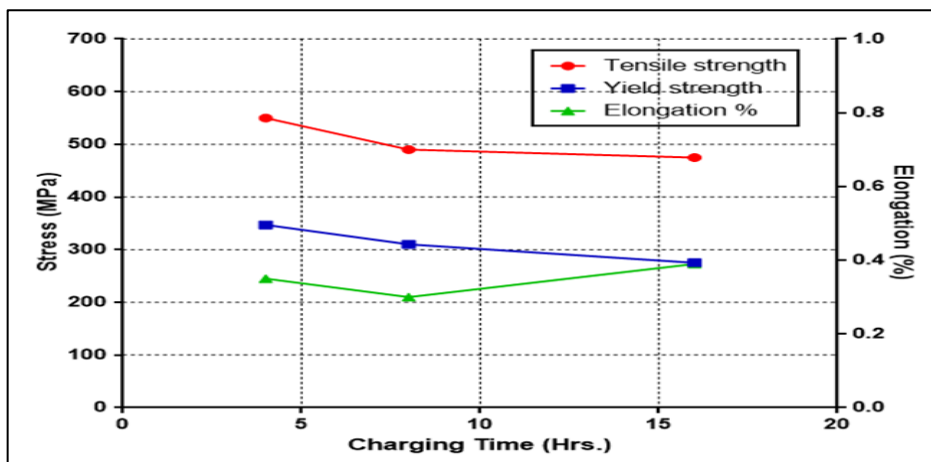


Figure 11: Effect of hydrogen charging on uncoated AISI-1018 Steel



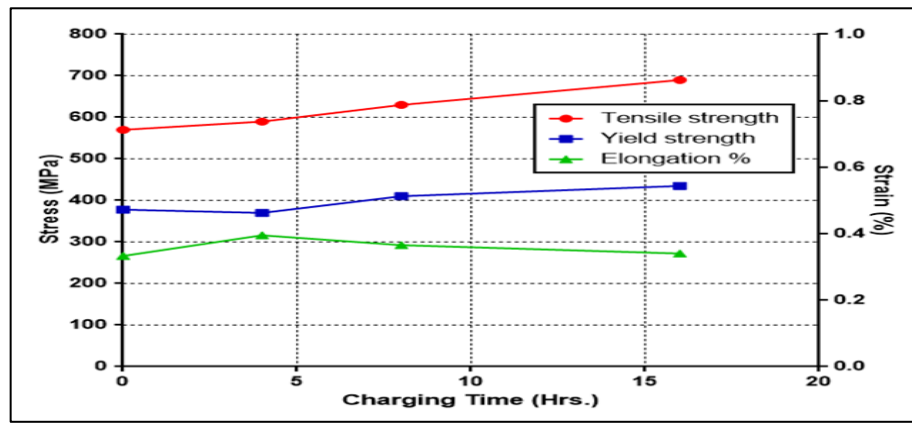


Figure 12: Effect of hydrogen charging on Titanium coating for AISI-1018 Steel

A decrease in tensile strength with a long charging time is shown in the red line. The effect is clear until the charging time exceeds 8 hours. The same can be applied to the yield strength. As for elongation, it can be seen that it decreased. Still, after 8 hours of charging, the elongation increased due to hydrogen permeation in bulk material leading to the degradation of metal stiffens due to the hydrogen embrittlement effect. This leads to mental strength loss. The above curves represent the natural effect of hydrogen permeation in steel.

After coating with the Titanium nano layer alone, the behavior of the base metal (i.e., steel AISI1018) increased yield and ultimate tensile strength, as shown in Figure 12. With a charging time of 4 hours, the yield strength remained steady, but the ultimate strength increased by 5%. At 8 hours of charging, both tensile and yield strength slightly decreased. Elongation also increased slightly after 8 hours. The above relations indicate that the material was strengthened by adding a nano Titanium coat with longer charging, up to 16 hours. The yield and tensile strengths increased together with little effect on elongation.

Comparing the effect of adding a Titanium nano layer using sputtering to a non-coated specimen shows an improvement in the base metal mechanical properties.

By adding a second coat layer of (TiO<sub>2</sub>+Al<sub>2</sub>O<sub>3</sub>) on the prior Titanium layer to the tensile specimens with different charging times, there was no change in properties after charging for 4 hours. Still, at 8 hours of charging, both yield and tensile strength improved dramatically, as shown in Figure 13.

With a long charging time of 16 hours on double-layer specimens, mechanical properties begin to degrade but remain above what was founded for uncoated charged specimens. In addition, the elongation conduct for double-layer nano-coating shows a continuous increase in charging time, which is different from single Titanium layer specimens.

Coating with triple-layer layer+(TiO<sub>2</sub>+Al<sub>2</sub>O<sub>3</sub>)+Al<sub>2</sub>O<sub>3</sub> on AISI-1018 Steel decreases mechanical properties, as shown in Figure 14. The tensile and yield strength and elongation degraded downside. This means that the triple coating failed to maintain at least acceptable mechanical properties against the Hydrogen charging effect. Moreover, it is worth mentioning that some of the coat peels began to appear microscopically after triple-layer coating. This may lead to removing the first and second layers leaving the steel surface without protection. Comparing these results to the results shown in Figure 11 for uncoated specimens, it is clear that the results were the same, meaning the triple-layer effect collapses the two other layers.

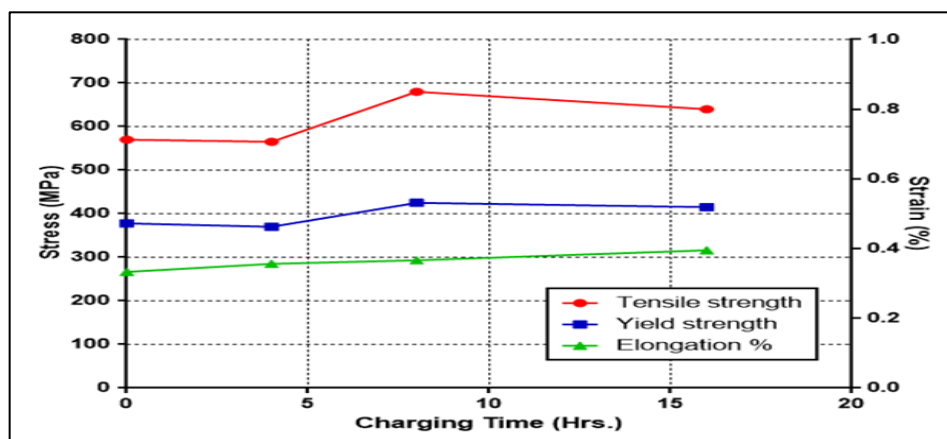
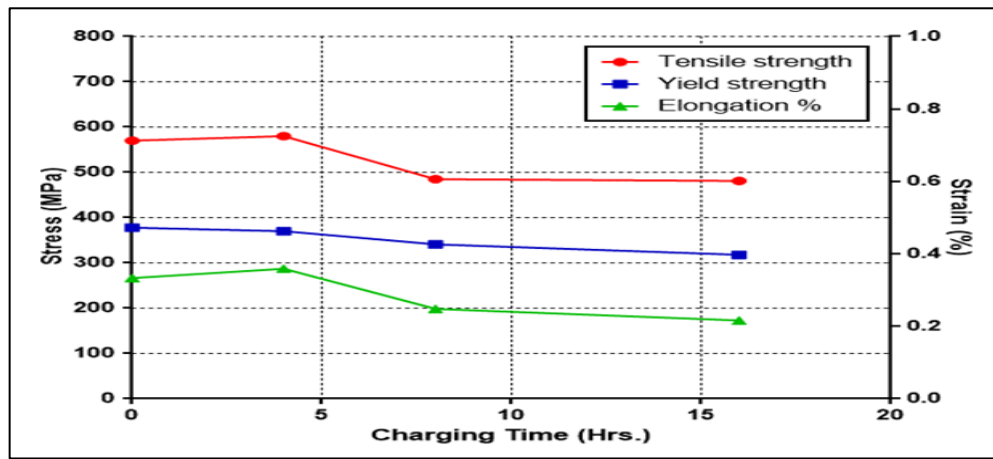


Figure 13: Effect of hydrogen charging by coating double layer Ti+(TiO<sub>2</sub>+Al<sub>2</sub>O<sub>3</sub>) on AISI-1018 Steel





**Figure 14:** Effect of hydrogen charging by coating triple layer  $+(TiO_2+Al_2O_3)+Al_2O_3$  on AISI-1018 Steel

From all the above, the best logical explanation that can be suggested is that the nano-coating by Titanium or Titanium and Aluminum oxides act as atomic sieves for hydrogen atoms to allow a minimum amount of atomic Hydrogen in steel structure. Then, the hydrogen atoms take interstitial locations in the lattice, causing internal stresses arising yield and tensile strength of steel with little effect on elongation. Therefore, they are distributed within the crystal lattice in a uniform and homogeneous manner. Hydrogen atoms occupy interstitial sites within the crystal lattice, leading to a distortion in it (Because the space inside the lattice is not enough to accommodate a solute atom without displacement of neighboring atoms). This distortion is the tension and compression energy between the iron and hydrogen atoms inside the metal, where the crystal structure was stable and the distance between the iron atoms was fixed, so when the hydrogen atoms enter, the iron atoms move away from each other; thus, the tensile and compressive forces generated, and this looks like a cold working inside the metal. [24, 25]

Although the coat application in this work does not include wear, adhesion is important to be investigated since it allows safe product handling without easy removal of the nano coat layer. The adhesion test is done by peeling the coat using the pull-off adhesion strength of coating ASTM D7234-12 standard. The maximum adhesion value related to the triple layer was found to be 596 psi (4.1 MPa). In addition, the lowest value was 309 psi (2.13 MPa) by coating with Ti alone.

**Table 4:** Adhesion Strength for a different layer for 5 hours

Specimens	Adhesion force (Psi)	Roughness average (nm)
Coated Ti	309	4.831
Coated (Ti)+ (0.75 $TiO_2$ +0.25 $Al_2O_3$ )	524	8.374
Coated (Ti) + (0.75 $TiO_2$ +0.25 $Al_2O_3$ ) + ( $Al_2O_3$ )	596	8.917

The magnitude of the adhesion strength for the coated first layer Ti, double-layer [ $TiO_2$ ,  $Al_2O_3$ ], and third  $Al_2O_3$  layer explain the strength of the bonds responsible for the Van der Waals forces adhesive mechanism between 1018 steel and coat layer. It is characterized by its effectiveness between adhesives and affixed—the chemical bonding forces that give a kind of adhesion strengthening that occurs when the adhesive contains chemical groups that interact with the material to be attached to it and mechanical interlocking forces. The results of roughness, listed in Table 4, showed that the surface roughness of a coating is directly proportional to the adhesive in addition to the titanium component of its properties that it is used as a coating.

It was found that the maximum adhesion value related to the triple layer was 596 psi (4.1 MPa). On the other hand, coating with Ti alone was the lowest at a value of 309 psi (2.13 MPa).

#### 4. Conclusions

Several findings can be drawn from the results and discussions presented in this study. The deposition of a single layer of Ti ( $TiO_2$  with  $Al_2O_3$ ) and triple-layer  $Al_2O_3$  on steel 1018 using DC sputtering can be summarized as follows:

- 1) Steel coating with high hydrogen nano barrier as Titanium or Aluminum raises the base metal mechanical properties and improves the steel structure selection for proper application.
- 2) The samples coated with (0.75  $TiO_2$ : 0.25  $Al_2O_3$ ) by the DC sputtering give the best hydrogen embrittlement resistance.
- 3) The maximum adhesion value related to the triple layer was 596 psi.
- 4) The bonding and adhesion between the Ti layer with ( $TiO_2$  &  $Al_2O_3$ ) ceramic coatings AISI 1018 carbon steel were acceptable in handling but not in wear applications.
- 5) The results of the surface roughness coating by the DC sputtering technique are proportional to the adhesive. The maximum adhesion value related to the triple layer was 596 psi.

### Author contribution

All authors contributed equally to this work.

### Funding

This research received no specific grant from any funding agency in the public, commercial, or not-for-profit sectors.

### Data availability statement

The data that support the findings of this study are available on request from the corresponding author.

### Conflicts of interest

The authors declare that there is no conflict of interest.

### References

- [1] R.N. Iyer, H.W. Pickering, Mechanism and kinetics of electrochemical hydrogen entry and degradation of metallic systems. *Annu. Rev. Mater. Sci.*, 20 (1990) 299-338. <https://doi.org/10.1146/annurev.ms.20.080190.001503>
- [2] R.P. Gangloff, Critical issues in hydrogen assisted cracking of structural alloys, Oxford Elsevier Science. 1 (2008) 141-165. <https://doi.org/10.1016/B978-008044635-6.50015-7>
- [3] M. M. Mirza, E. Rasu, A. Desilva, Influence of Nano additives on Protective Coatings for Oil Pipe Lines of Oman, *Int. J. Chem. Eng. Appl.*, 7 (2016) 221-224. <https://doi.org/10.18178/ijcea.2016.7.4.577>
- [4] M. J. Kadhim, K. A. Sukkar, Investigation Nano coating for Corrosion Protection of Petroleum Pipeline Steel Type A106 Grade B. Theoretical and Practical Study in Iraqi Petroleum Sector, *Eng. Technol. J.*, 35 (2017) 1042- 3413.
- [5] Q. J. Sulaiman, A. Al – Taie, D.M. Hassan, Evaluation of Sodium Chloride and Acidity Effect on Corrosion of Buried Carbon Steel Pipeline in Iraqi Soil, *Iraqi J. Chem. Pet. Eng.*, 15 (2014) 1-8. <https://doi.org/10.31699/IJCPE>
- [6] C. Matteo, Current and Future Nanotech Applications in the Oil Industry, *Am. J. Appl. Sci.*, 9 (2012) 784-793. <https://doi.org/10.3844/ajassp.2012.784.793>
- [7] T. Michler, J. Naumann, Influence of high-pressure hydrogen on the tensile and fatigue properties of a high strength Cu–Al–Ni–Fe alloy, *Int. J. Hydrogen Energy*, 35 (2010). <https://doi.org/10.1016/j.ijhydene.2010.07.093>
- [8] G. Balakrishnan, Effect of substrate temperature on microstructure and properties of nano crystalline titania thin films prepared by pulsed laser deposition, *Nanosys. Phys. Chem. Math.*, 7 (2016) 621–623. <http://dx.doi.org/10.17586/2220-8054-2016-7-4-621-623>
- [9] H.J. Cialone and J.H. Holbrook. Sensitivity of Steels to Degradation in Gaseous Hydrogen, In: *Hydrogen Embrittlement: Prevention and Control*, ASTM STP 962, L. Raymond (Ed.), 134-152, 1988. <https://doi.org/10.1520/STP45297S>
- [10] A. Barnoush, H. Vehoff, Recent developments in the study of hydrogen embrittlement: Hydrogen effect on dislocation nucleation. *Acta Mater.*, 58 (2010) 5274-5285. <https://doi.org/10.1016/j.actamat.2010.05.057>
- [11] J. Song, W.A. Curtin, Atomic mechanism and prediction of hydrogen embrittlement in iron. *Nat. Mater.*, 12 (2013) 145–151. <https://doi.org/10.1038/nmat3479>
- [12] H.K. Birnbaum, Hydrogen effects on deformation and fracture, science and sociology. *MRS Bull.*, 28 (2003) 479-485. <https://doi.org/10.1557/mrs2003.143>
- [13] M. Dadfarnia, P. Novak, D. C. Ahn, J. B. Liu, P. Sofronis, D. D. Johnson at all. Recent advances in the study of structural materials compatibility with hydrogen. *Adv. Mater.*, 22 (2010) 1128-1135. <https://doi.org/10.1002/adma.200904354>
- [14] Y. Katz, N. Tymiak, W.W. Gerberich, Nanomechanical probes as new approaches to hydrogen/deformation interaction studies. *Eng. Fract. Mech.*, 68 (2001) 619-646. [https://doi.org/10.1016/S0013-7944\(00\)00119-3](https://doi.org/10.1016/S0013-7944(00)00119-3)
- [15] Gerberich WW, Marsh PG, Hoehn JW. Hydrogen induced cracking mechanisms. In: Moody NR, Hoehn JW, editors. *Hydrogen effects in materials*. Warrendale, PA: TMS, 1996.
- [16] H. M. Jedy, R.A. Anae, Characterization of Nb<sub>2</sub>O<sub>5</sub>-Ni Coating Prepared by DC Sputtering, *Eng. Technol. J.*, 39 (2021) 565-572. <https://doi.org/10.30684/etj.v39i4A.1902>
- [17] A. Shanaghi, A. S. Rouhaghdam, M. Aliofkhaezrai, Study of TiO<sub>2</sub> nanoparticle coatings by the SOL-GEL methods for corrosion protection, *Mater. Sci.*, 44 (2008) 233-246. <https://doi.org/10.1007/s11003-008-9070-6>
- [18] M.A. Deyab, S.T. Keer, Effect of nano-TiO<sub>2</sub> particles size on the corrosion resistance of alkyd coating. *Mater. Chem. Phys.*, 146 (2014) 406-411. <https://doi.org/10.1016/j.matchemphys.2014.03.045>

- [19] T.Eguchi, M.Tamura, Nanostructured thin films for hydrogen-permeation barrier, *J. Vac. Sci. Technol., A: Vac. Surf. Films*, 33 (2015) 041503. <https://doi.org/10.1116/1.4919736>
- [20] X. Li ,L.Chen, H. Liu,C. Shi, D. Wang ,Z. Mi and L.Qiao, Prevention of Hydrogen Damage Using MoS<sub>2</sub> Coating on Iron Surface, *Nanomater.*, 9 (2019) 1-10. <https://doi.org/10.3390/nano9030382>
- [21] M.Wasim, M. B. Djukic, Hydrogen embrittlement of low carbon structural steel at macro-, micro- and nano-levels. *Int. J. Hydrog. Energy.*, 45 (2020) 2145-2156. <https://doi.org/10.1016/j.ijhydene.2019.11.070>
- [22] Autoren, C. Wegst, M. Wegst, Key to steel, part 1, 2004.
- [23] ASTM E8-04 , Standard Test Methods for Tension Testing of Metallic Materials, American Association State. 2010.
- [24] D. L. Liu, J. Martin, and N. A. Burnham, Optimal roughness for minimal adhesion, *Appl. Phys. Lett.*, 91 (2007) 043107. <https://doi.org/10.1063/1.2763981>
- [25] S. Ayadi, Y. Charles, M. Gaspérini, I. C.Lemaire, T. D. S. Botelho, Effect of loading mode on blistering in iron submitted to plastic prestrain before hydrogen cathodic charging, *Int. J. Hydrog. Energy.*, 42 (2017) 10555-10567 <https://doi.org/10.1016/j.ijhydene.2017.02.048>